DESIGN AND CONFIGURATION CONTROL OF SPACE ROBOTS UNDERGOING IMPACT

Evangelos Papadopoulos, Iosif Paraskevas

Department of Mechanical Engineering, National Technical University of Athens, Athens 15780, Greece
egpapado@central.ntua.gr, iparaskevas@central.ntua.gr

ABSTRACT

The necessity of robot manipulators in space is a one-way reality. The aim of this research work is to produce guidelines for grasping objects on orbit with the use of a space manipulator, such that manipulator reaction forces are minimized and therefore minimum disturbance forces are transmitted to its base. Impact reaction forces appear during the contact of two bodies. A methodology that uses the property of the *percussion point* of bodies that can rotate around a fixed axis is presented. The equations that describe the percussion point are developed. These functions are studied in depth to predict the best configuration of a manipulator during impact. A number of simulations are executed in order to examine the validity of these predictions, and guidelines suggesting optimal approach configurations are proposed.

1. INTRODUCTION

The commercialization of space introduces the need for robotic devices that can assist humans in the construction, repair, protection and maintenance of space stations or satellites. To increase the mobility of such devices, free-flying systems in which one or more manipulators are mounted on a thruster-equipped spacecraft, have been proposed and flown, see Fig. 1.

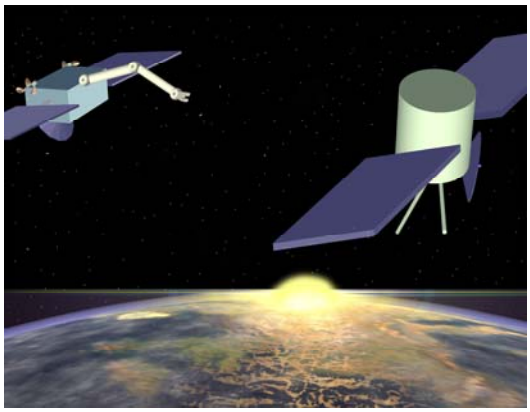

Figure 1. Artist's rendition of robotic capture on orbit.

The usefulness of robots has been recognized by space agencies around the world and has led to research and/or construction of systems such as the European Robotic Arm and the RMS for the ISS, the Canadarm for the Space Shuttle, or the Japanese ETS-7, to name a few of them. An in depth investigation of the areas that a robot system can be used, exists in a small number of documents (Waltz, 1993 and Ellery, 2000). A robot in space can assist in repairing and therefore extending the life of space systems. It can also help in removing dangerous debris from the orbital environment. Other uses include the construction of large scale systems in orbit, the participation in life rescue missions and last but not least, the technology transfer of the state-of-the-art to terrestrial systems. The economic potential of all these aspects is enormous and difficult to put aside.

Space robots are described by complex dynamics and are subject to conditions such as the lack of gravity, and of a fixed base. A number of previous research works have focused on docking, planning, dynamics and control, etc. (Ellery, 2000). However, the issue of reaction minimization due to docking impacts has not been studied adequately. Optimal trajectory for capture targets avoiding collision between the chaser robot and the targeted object has been presented (Jacobsen et. al., 2002). A cautious approach can reduce the effects of an impact, but in general, it cannot eliminate the development of reaction forces at the joints of the robot manipulator, and through propagation, to the base. Recent work investigated the dynamics of the system chaser-target in order to find how much these can be pushed away at the docking phase (Yoshida et. al., 2003). The stability and performance of a space system has been examined for a space robot with of on-off thrusters and a technique of reducing fuel consumption has been proposed (Martin et. al., 1996). The reaction moment effect of satellite-based manipulators and the feasibility of stabilizing the base platform during arm operations has been studied (Carignan, Akin, 2000). Research work also has been presented for free-floating systems where the spacecraft moves in response to manipulator motions, (Papadopoulos, Dubowsky, 1993) or for planning smooth trajectories for such systems (Papadopoulos et. al. 2005 and Papadopoulos and Nanos, 2004).

This study tries to generate a different way of dealing with these situations, using the same impact itself as a

Proceedings of the 6th International ESA Conference on Guidance, Navigation and Control Systems, Loutraki, Greece, 17-20 October 2005 (ESA SP-606, January 2006)

way to eliminate (as far as it is possible) its effects. Minimizing reaction forces results in more capable systems and reduces the amount of thruster fuel required to keep the system under control. Obviously, reduced fuel consumption increases the life of a space robot and is therefore very desirable. The basis of this methodology is the exploitation of the notion of the percussion point that will be presented thoroughly.

First, a brief discussion of common docking strategies is presented. A planar analysis of the theory of the percussion point is presented next. The fundamental equations are illustrated with examples that show the advantages of a controlled impact at the percussion point. This kind of controlled impact can work efficiently as a filter of the translational forces that are propagated through the links to the base, only by the appropriate configuration of the robot. By this technique, the effect of an impact to the base link is minimized.

The dynamics of space robots under impacts are considered next. A simple two-link planar robot system with revolute joints and a free flying base is used as an example. Its dynamics are derived through a recursive Newton-Euler algorithm that allows the direct computation of system internal forces and torques in real time. The code is created in Mathematica code and the dynamics are integrated in Matlab/Simulink. A number of simulations run to study the validity of the assumptions created in connection with the Center of Percussion. A number of different configurations of the space robot are considered which were chosen following the analysis of the theory of percussion point. The impact is examined at different positions of the two revolute links, and for different angles of the force direction with the axis of the last link. Additionally, a number of intermediate joint locations are examined in order to find the optimal space manipulator configuration during impact.

The system is studied in three basic modes. In the first, the base is able to move freely without using thrusters and the joints are free of actuator torques. In the second mode, the joints are controlled with model-based PD type-controllers that try to eliminate the effects of the impact, while in the third mode the joints are assumed to be fixed due to the existence of gearboxes with large gear ratios. Through an extensive number of simulation experiments, we show that the applicability of the theory of percussion point is ensured and its exploitation offers distinct advantages. The study points out that with a clever design of a robot from the very beginning, and the appropriate planning and control systems, many impacts can be successfully filtered without additional hardware. Finally, a number of guidelines are proposed in order to help in the design of future robotic systems in space.

2. DOCKING STRATEGIES

The main focus of this paper is the impact during capture of a target. However, to reach this point, a system must follow a docking/ capturing strategy. Such strategies are presented here briefly. The repairing/ capturing vehicle is referred to as the chaser, while the vehicle to be repaired or the debris are referred to as the target. Docking strategies have been proposed by Yoshida K., et al., 2004, Jacobsen S., et al., 2002 to name a few.

Generally, the docking phase consists of five steps. First, the chaser acknowledges that there is a problem with a spacecraft. Through ground control and its own sensors, it acquires information about the target's characteristics. Next, the chaser gets closer and attempts to have the same motion as that of the target. In the sequel, using a manipulator, it grasps the target and, if needed, attempts to stabilize it. Next, one or more manipulators work on the target, and finally, the target is released away from the repaired vehicle with caution.

The grasping phase that interests this study most, presents a number of difficulties since a large number of satellites and other space structures do not have a docking point. Two strategies commonly used include using the nozzle of the apogee kick motor and the payload attachment fitting. However, independent of the docking method employed, the robotic manipulator will have to deal with a number of forces and impulses generated from the fact that two bodies of large inertia, mass and velocity come in contact.

The case of capturing debris is somehow different. Debris definitely have no docking points and may have diverse sizes and geometries. In this case, an impact may occur during deceleration of the debris by the capturing manipulator. The manipulator may work here as a bat trying to change the track of an object so that it becomes feasible to capture it using a special end-effector or another manipulator.

In both capturing cases, impacts between the chaser manipulator(s) and the target will occur. To deal with these, we examine next the concept of the center of percussion.

3. THE PERCUSSION CENTER CONCEPT

3.1. Theory of Percussion Point

The Percussion Point or else the Center of Percussion (COP) is a property of all bodies able to rotate about a

fixed axis. The interesting property of this point is that, if an impact occurs on such a body at the COP, the reaction force which is exerted on the fixed rotation axis tends to a minimum value, including zero. The COP is not unknown in mechanics, but it has been of little use so far. Because of this, the concept is not widely known and its analytical description in the bibliography is scarce.

To understand its properties, we consider a beam that can rotate around an axis normal to its longitudinal axis, see Fig. 2.

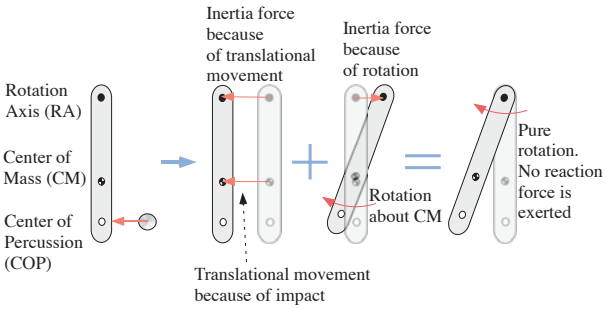

Figure 2. The concept of the Percussion Point.

Suppose an impact occurs at a point as shown in Fig. 2. The overall movement of the body consists of two movements. The first motion is translational, while the second is rotational. During the first motion, the body tries to move in the direction of the impulse, therefore an inertial force is exerted at its fixed point. Simultaneously, the body rotates around its Center of Mass (CM), thus exerting an inertial force at the fixed point, at a direction opposite to that of the previous one. The vectorial sum of the forces exerted on the pin joint is the reaction force during the impact. One can now define the COP as that particular point which will produce a zero reaction force, at least theoretically.

Next, we consider the free body diagram shown in Fig. 3. Assuming an impact force at some point along the longitudinal axis, the reaction forces are computed. For purposes of generality, the impact force can have any direction. Gravitational forces are still counted but as will be soon evident, they do not affect the result.
Balance of forces and of moments yield

$$m \cdot \ddot{x}_{cm} \cdot \cos\theta = N_x - F \cdot \sin(\theta + \phi) \quad (1)$$

$$m \cdot \ddot{y}_{cm} \cdot \sin\theta = N_y - m \cdot g + F \cdot \cos(\theta + \phi) \quad (2)$$

$$I_o \cdot \ddot{\theta} = -m \cdot g \cdot r_{cm} \cdot \sin\theta + F \cdot \cos(\theta + \phi) \cdot l \cdot \sin\theta - \\ -F \cdot \sin(\theta + \phi) \cdot l \cdot \cos\theta \quad (3)$$

where all symbols are defined in Fig. 3. Integrating all parts for a small fraction of time according to the following equation

$$\lim_{\varepsilon \to 0} \int_0^{\varepsilon} f(x)dt \quad (4)$$

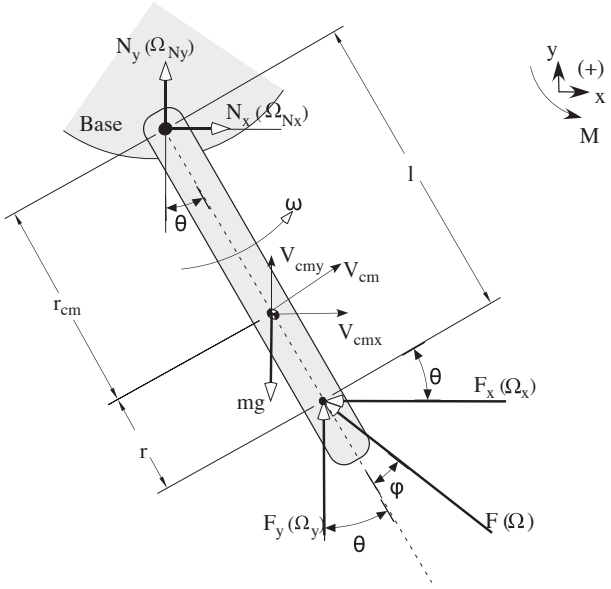

Figure 3. Free body diagram for the COP analysis.

yields the following the result,

$$m \cdot x_{cm} \cdot \cos\theta = \Omega_{Nx} - \Omega \cdot \sin(\phi + \theta) \quad (5)$$

$$m \cdot y_{cm} \cdot \sin\theta = \Omega_{Ny} + \Omega \cdot \cos(\phi + \theta) \quad (6)$$

$$I_o \cdot \dot{\theta} = \Omega l \sin\theta \cos(\phi + \theta) - \Omega l \cos\theta \sin(\phi + \theta) \Rightarrow$$

$$\Rightarrow I_o \cdot \dot{\theta} = \Omega l \left[\sin\theta \cos(\phi + \theta) - \cos\theta \sin(\phi + \theta) \right] \Rightarrow$$

$$\Rightarrow I_o \cdot \dot{\theta} = -\Omega \cdot l \cdot \sin\phi \quad (7)$$

where Ω is the impulse of the corresponding force (for example $N_x \rightarrow \Omega_{Nx}$). Since,

$$I_o \cdot \dot{\theta} = I_o \cdot \omega = I_o \cdot \frac{v_{cm}}{r_{cm}} = -\Omega \cdot l \cdot \sin\phi \Rightarrow$$

$$\Rightarrow v = -\frac{\Omega \cdot l \cdot r}{I} \cdot \sin\phi \quad (8)$$

hence, the impulse components are given by,

$$\Omega_{Nx} = \Omega \cdot \left(\sin(\phi + \theta) - \frac{l \cdot r_{cm} \cdot m}{I_o} \cdot \cos\theta \cdot \sin\phi \right) \quad (9)$$

$$\Omega_{Ny} = \Omega \cdot \left(-\cos(\phi + \theta) - \frac{l \cdot r_{cm} \cdot m}{I_o} \cdot \sin\theta \cdot \sin\phi \right) \quad (10)$$

Using Eqs. (9) and (10), the magnitude of the impulse is given by,

$$\Omega_N{}^2 = \Omega^2 \cdot \left[1 + \left(\alpha^2 - 2 \cdot a \right) \cdot \sin^2 \phi \right] \quad (11)$$

with

$$a = \frac{l \cdot r_{cm} \cdot m}{I_o} \quad (12)$$

It must be noted that the above result does not depend on the value of θ, which means that the initial angle of the bar has no effect on the magnitude of the impulse and consecutively on the reaction force.

In order to found the COP, Ω must be zero. Using Eq. (11), we can readily compute that ϕ must be given by

$$\phi = \pm Arc\sin\left(\frac{1}{\sqrt{2 \cdot a - a^2}} \right) \quad (13)$$

It can be seen that this happens only if a=1 and $\phi = \frac{\pi}{2}$.

Using Eq. (12), the fact that the inertia of the body around the rotation axis is

$$I_o = I_{cm} + m \cdot r_{cm}{}^2 \quad (14)$$

and, that

$$l = r_{cop} + r_{cm} \quad (15)$$

it can be found that the location of the COP is given by

$$r_{cop} = \frac{I_{cm}}{r_{cm} \cdot m} \quad (16)$$

We can now make the following remarks. If $r_{cm} = 0 \Rightarrow r_{cop} = \infty$, that is, if the rotation axis coincides with the CM, then the COP tends to infinite. Practically the reaction forces cannot be zeroed in this case. If $r_{cop} = 0 \Rightarrow r_{cm} = \infty$, that is, if the rotation axis is far from the CM, then the COP tends to coincide with the center of mass.

Fig. 4 displays the minimum of reaction impulses (and consequently forces) under various configurations. It can be seen that the minimum occurs for α=1 and ϕ=90°, and in general the nearer α and ϕ are to these values, the smaller a reaction is exerted.

An additional remark is that the COP is not actually one single point, but the same property is shared by all points along the line of impact (that is the direction at which the force impacts the beam). This line is normal to the body longitudinal axis defined as the line which passes through the pin joint and the body CM.

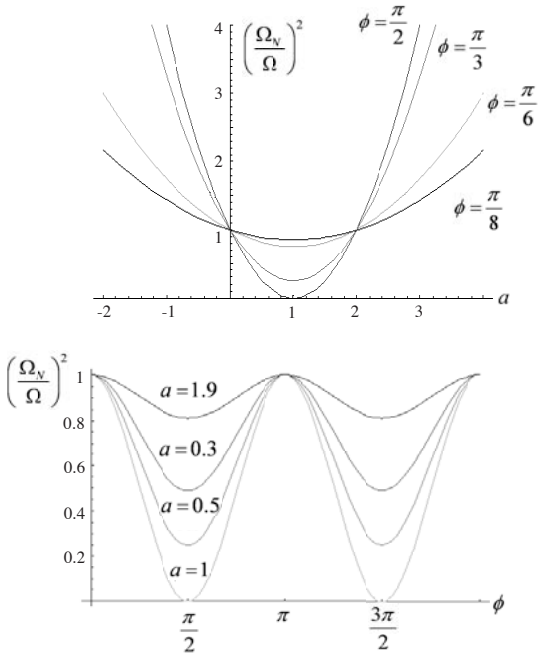

Figure 4. (a) Reaction impulse as a function of α for different ϕ's; (b) Reaction impulse as a function of ϕ for different α's.

3.2. The use of COP in consecutive rotational joints

As seen above, joint reaction forces are minimum when the impact occurs at the COP and at a 90° angle with respect to the longitudinal axis of the beam. This can be extended to a robot manipulator, because links can be considered as beams. In the case of a space robot, no fixed axis exists. However, due to the small duration of the impact and the relatively large inertia of the base with respect to the links, the previous analysis still holds.

Up to this point, single beams were considered. Next, the case of a serial multiple-link planar manipulator with revolute joints, see Fig. 5, is examined. A force acts at the COP of link n in some direction. Since the force is not necessarily normal to the link's longitudinal axis, the x-component reaction is eliminated but the y-component reaction is not. If the impact does not occur exactly at the COP, then even the x-component will not

be eliminated completely. Assume that a fraction ε_n of the reaction force appears at joint n. Now if joint n is attached at link's n-1 COP, then the y-component can be filtered up to a small proportion ε_{n-1}, but the x-axis component from the reaction will still remain and transmitted further. If a number of consecutive revolute joints are considered, it is evident that the last joint which is attached at the base will experience an impact force which will be very small. Based on these remarks, it is evident that two revolute joints is the minimum for 2D cases, and three revolute joints for 3D cases. This analysis gives a general idea of what simulations or experiments are expected to show.

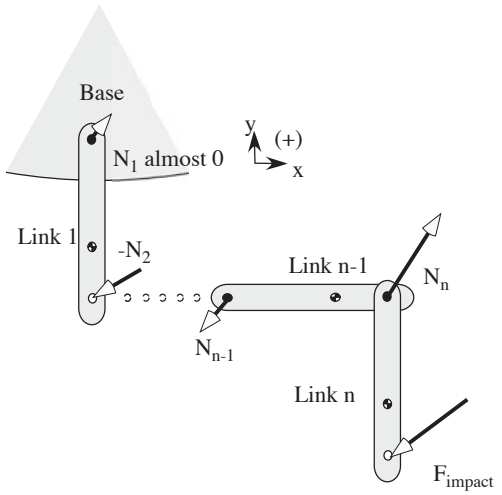

Figure 5. Space robot with consecutive links.

3.3. Derivation of COP equations through a Newton-Euler Algorithm

The COP can be derived using the Newton-Euler Algorithm (NEA). The exact algorithm can be easily found in most robotics textbooks. The notation used in NEA is shown in Fig. 6 for link i.

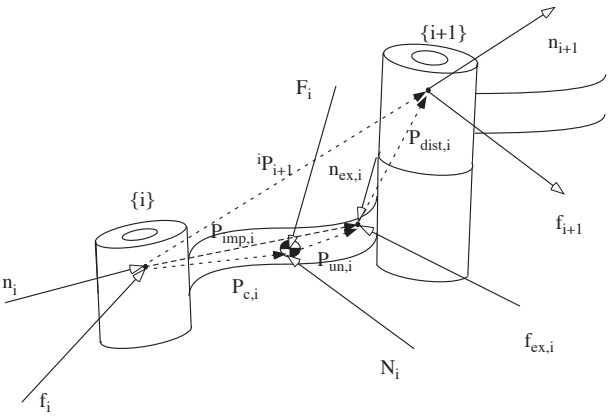

Figure 6. Values for Newton-Euler Algorithm.

The moment equation for link i, integrated over (small) time is

$$\left({}^{\mathbf{i}}\mathbf{P}_{\mathbf{C,i}} + {}^{\mathbf{i}}\mathbf{P}_{un,\mathbf{i}}\right)\times {}^{\mathbf{i}}\boldsymbol{\Omega}_{\mathbf{f,i}} =$$
$$\overbrace{\left[{}^{\mathbf{i}}\mathbf{P}_{un,\mathbf{i}}\times\left(m_i\cdot {}^{\mathbf{i}}\mathbf{u}_{\mathbf{i}}\right)+\int\left({}^{\mathbf{i}}\mathbf{n}_{\mathbf{i}}-{}^{\mathbf{i}}_{\mathbf{i+1}}\mathbf{R}\cdot {}^{\mathbf{i+1}}\mathbf{n}_{\mathbf{i+1}}+{}^{\mathbf{i}}\mathbf{n}_{\mathbf{ex,i}}\right)\right]}^{\langle A\rangle}+$$
$$+\underbrace{\left[{}^{\mathbf{i}}\mathbf{P}_{un,\mathbf{i}}\times m_i\cdot\left({}^{\mathbf{i}}\boldsymbol{\omega}_{\mathbf{i}}\times {}^{\mathbf{i}}\mathbf{P}_{C,\mathbf{i}}\right)-{}^{\mathbf{C,i}}\mathbf{I}_{\mathbf{i}}\cdot {}^{\mathbf{i}}\boldsymbol{\omega}_{\mathbf{i}}\right]}_{\langle B\rangle}-$$
$$-\underbrace{\left[{}^{\mathbf{i}}\mathbf{P}_{dist,\mathbf{i}}\times {}^{\mathbf{i}}_{\mathbf{i+1}}\mathbf{R}\cdot {}^{\mathbf{i+1}}\boldsymbol{\Omega}_{\mathbf{f,i+1}}\right]}_{\langle C\rangle} \qquad (17)$$

We are interested to have joint impulses equal to zero. Then terms A, B, and C in Eq. (17) must all be zero. Since the initial translational velocity of all joints is zero, then the first term in term A is zero. Also, the integral is zero because of the small duration of impact and the assumption that the configuration does not change for small time. The B term is the equation that gives the COP. For term C to be zero, link i-1 must be joined at COP of link i. In other words, this last term shows that in general can act at the link an impact force and reaction from the previous link (i+1). However in order not to have reaction forces in bearings of link i, these two forces must act at the same position, the COP of link i, and therefore ${}^{\mathbf{i}}\mathbf{P}_{dist,\mathbf{i}}$ must be zero. On the other hand, this means that the impact force acts directly on the bearings of link i+1. This is the reason why in the following analysis one force acts at a link at any time, either this is the impact, or the reaction force from the previous link.

4. SYSTEM DESCRIPTION AND DYNAMICS

4.1. Description of the system

The 2D system under investigation consists of a thruster-equipped base, able to make x-y translational planar motions and a rotational motion around the z axis. The manipulator consists of two links connected by rotational joints able to rotate around the z axis, too. The full system has five degrees of freedom (DOF), as shown in Fig. 7.

The end effector can be at the tip of the last link or at some other point (for example at the calculated COP). Table I displays the physical properties of the system to be simulated, including the position of COP for the two rotational links, calculated with the use of Eq. (16). To apply the NEA, two virtual translational links with directions along the inertial x and y axis have been implemented. The second virtual link points to the base CM.

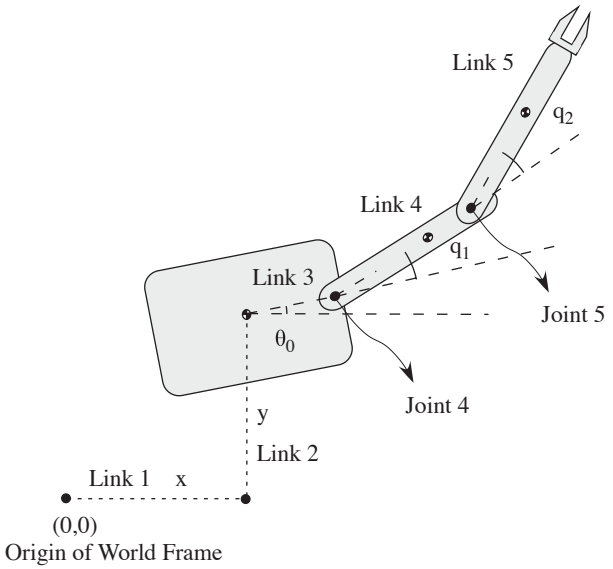

Figure 7. The Space System and its DOFs.

Table 1. Physical characteristics of system.

Link	Mass (kg)	Inertia ($kg\text{-}m^2$)	Joint length l_i (m)	Center of Mass position from origin of local coordinates l_{cmi} (m)	COP position from origin of local coordinates (m)
1	0	0	0	0	-
2	0	0	0	0	-
3	400	66.67	1	0	-
4	40	3.33	1	0.5	0.6665
5	30	25	1	0.5	0.6667

Note that the robot dynamics can be written in principle using a Lagrangian formulation, but these are not well-suited in calculating internal system forces, such as reaction forces at the joints. On the other hand, the NEA, although more complicated, can produce directly these forces, not to mention that in addition to this, this algorithm is more computer-orienteted.

The NEA algorithm was implemented in Mathematica, and the forces exerted by the system's actuators are produced. The classical NEA uses as initial conditions the translational and angular velocities of all DOFs, and the force exerted from the end effector to the environment at the tip of the last link. To simulate possible impacts at any point of the space robot, the NEA was modified to include external forces acting from the environment to each link and the base. Therefore, the equations of motion included all external forces acting at various robot points and a Jacobian matrix for resolving these at the system joints has been derived.

Based on the above remarks, the equation of motion of the system was found to have the form,

$$\boldsymbol{\tau} = \mathbf{M} \cdot \ddot{\mathbf{q}} + \mathbf{V}(\mathbf{q}, \dot{\mathbf{q}}) + \mathbf{J}^T \cdot \mathbf{F} \qquad (18)$$

where $\mathbf{q}$ is the vector of joint variables, $\boldsymbol{\tau}$ is the vector of actuator forces and torques, $\mathbf{M}$ is the configuration dependent mass matrix, $\mathbf{V}(\mathbf{q}, \dot{\mathbf{q}})$ is the vector of nonlinear velocity terms and $\mathbf{J}^T \cdot \mathbf{F}$ includes the effect of external impact forces $\mathbf{F}$ to each joint.

After the creation of the general dynamic equation and their transfer to the Matlab/Simulink environment, the model of the system has been built, as shown in Fig. 8. It is a simple model but there were readings of a great number of data in order to derive the results, such as velocities and accelerations of all joints (translational and rotational), position of the center of mass of the base, and of course the reaction forces at the two rotational joints, measured at the local frame coordinates (which interests more) and at world frame coordinates. All this data was also saved in matrices for further processing.

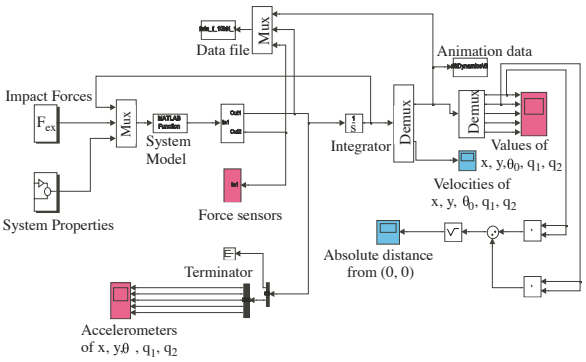

Figure 8. The Simulink model.

4.2. Setups and modes

The simulations were executed for seven different system configurations as displayed in Fig. 9.

Since the mobility of each joint is important in whether reaction forces can be transferred or not to another body, all seven configurations were studied in three distinct control modes affecting this mobility. The three control modes include (a) no control with direct actuation, (b) Model-based Control with direct actuation, (c) geared actuation mode.

(a) No Control, direct actuation: The manipulator joints are directly actuated, i.e. no gearboxes are present. Here, the actuators of the robotic system are turned off and no control is exercised over its joints. The base is in

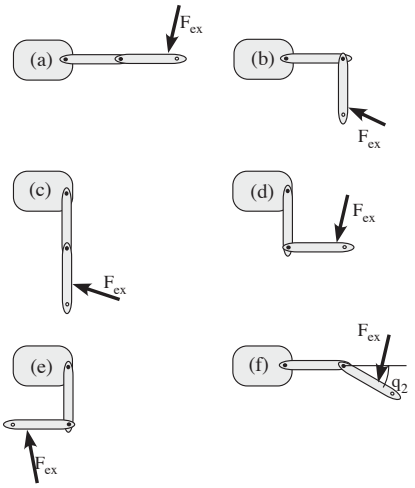

Figure 9. Initial conditions for q_1 and q_2. At case (f) q_2 takes two values.

free-floating mode, and the manipulator joints free to move. When an impact occurs the system moves according to its own dynamics. In this case, Eq. (18) is written as

$$\ddot{\mathbf{q}} = -\mathbf{M}^{-1} \cdot \mathbf{V}(\mathbf{q}, \dot{\mathbf{q}}) - \mathbf{M}^{-1} \cdot \mathbf{J}^T \cdot \mathbf{F} \qquad (19)$$

(b) Model Based Control, direct actuation. Again, the manipulator joints are directly actuated and no gearboxes are present. However, all degrees-of-freedom are position controlled, employing a model-based controller. The control law is given by Eq. (20):

$$\boldsymbol{\tau} = \hat{\mathbf{M}}(\mathbf{q}) \cdot \ddot{\mathbf{q}}^* + \hat{\mathbf{V}}(\mathbf{q}, \dot{\mathbf{q}}) \qquad (20a)$$

with

$$\ddot{\mathbf{q}}^* = \ddot{\mathbf{q}}_d + \mathbf{K_d} \cdot (\dot{\mathbf{q}}_d - \dot{\mathbf{q}}) + \mathbf{K_p} \cdot (\mathbf{q}_d - \mathbf{q}) \qquad (20b)$$

where the requirement is that the system following the impact must be controlled to its initial attitude and position with no velocity and no acceleration. The gains of the controllers were found so that the system error response is critically damped and shows an appropriate bandwidth as $K_p = 2.25$ and $K_d = 3$.

(c) Geared actuation: The base is free to move (free-floating system), but manipulator joints include a gearbox and are actuated using a model based control. The equation of motion has the form of Eq. (19), but now the two lower diagonal mass matrix elements are reduced by the square of the gear ratios and motor inertias are added, while other mass matrix are reduced by the gear ratios or their products, depending on the element's position. Other equation of motion terms are also reduced depending on their position. The physical result here is that the links are basically not backdriveable and the important dynamics are those of the motors themselves. The inertias of the motors are

$$\mathbf{I_{motor,4}} = 0.0005 Kgm^2 \,,\, \mathbf{I_{motor,5}} = 0.001 Kgm^2 \qquad (21)$$

and the two sets of gear ratios used in the simulations are,

$$n_4 = 30 \,,\; n_5 = 20 \qquad (22)$$

and

$$n_4 = 70 \,,\; n_5 = 60 \qquad (23)$$

4.3. External forces

The external force acts at the last link. The impact angle ϕ, impact position, joint position of joint 5 or the active control system, are changing each time in order to study how the response of the system differs. In all cases tried, the external force retains its direction during the fraction of time that this force affects the system. However, during this time the link may rotate under the force's effect and therefore the force may act on the link at a slightly different angle during this small fraction of time.

Finally the fraction of time is set equal to 0.01s, and its absolute amplitude is set equal to 10kN, so that the effect of the COP becomes more obvious.

5. SIMULATION RESULTS

What follows is a small number of typical plots selected from a great number of plots that were produced. A few things must be noted here. First, it was most convenient to plot forces and not impulses. The impulses can be found by multiplying the force exerted with the time duration of the impact. Secondly some of the modes discussed and showed in Fig. 9, are not presented here due to space limitations, but all necessary information is given.

5.1. Validation of the Center of Percussion notion

As it can be seen in Fig. 10, the minimum reaction force at joint 5 is exerted when the impact occurs exactly at the COP and with a 90^o impact angle. This happens for all cases, no matter what the initial attitude is or what control scheme is used. The behavior of joint 5 is actually the behavior of the body in Fig. 3.

5.2. Comparison between different initial attitudes

Examining next Fig. 11, it is obvious that the configurations with links in normal position to each other, give distinct advantages and no matter what the impact angle is, the system filters by itself the effects of the impact as far as joint 5 is at the COP of link 4 as a result of Section 5.1.

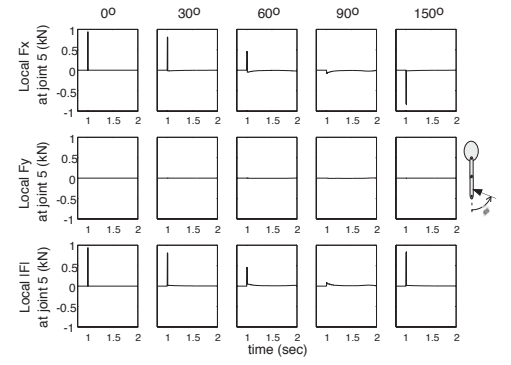

(a)

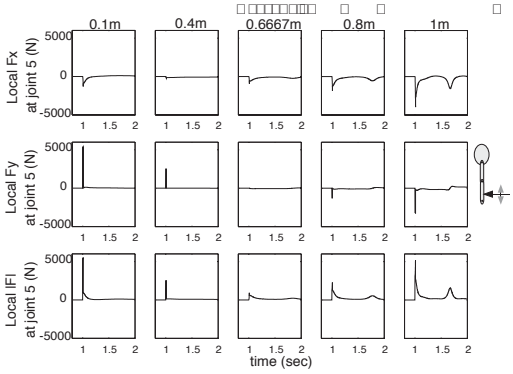

(b)

Figure 10. Reaction forces at the 5th joint for different (a) impact angle, (b) impact position.

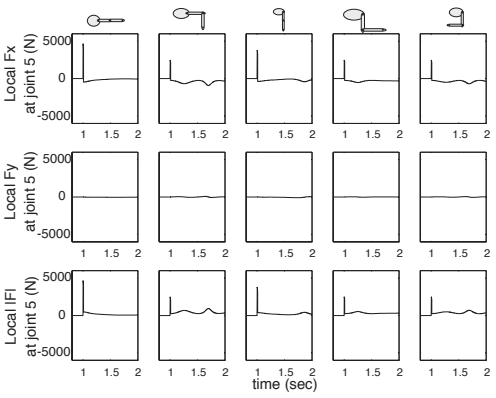

(a)

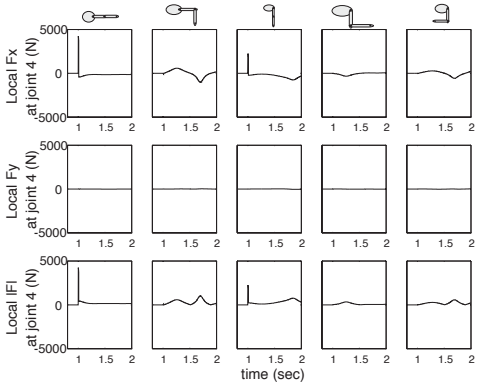

(b)

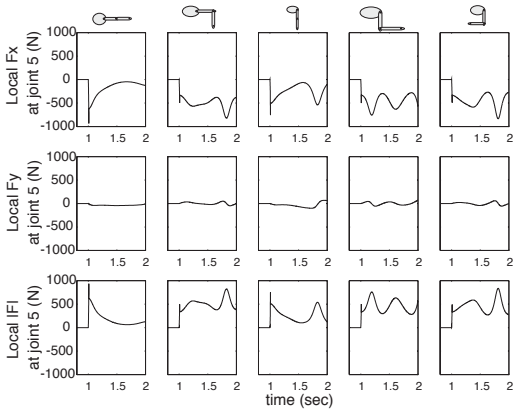

(c)

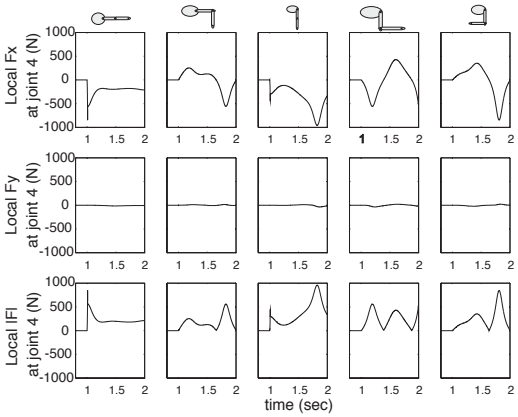

(d)

Figure 11. Attitudes of Fig. 9. Reaction at (a) Joint 5, impact angle (i.a.) $\phi = 60^o$; (b) Joint 4, i.a. $\phi = 90^o$; (c) Joint 5, i.a. $\phi = 90^o$; (d) Joint 4, $\phi = 90^o$.

Of course, if the impact occurs at a different position than the COP, a small fraction of it will not vanish (and therefore, the existence of a third revolute link can assist in filtering). However, compared to other configurations, the reactions are less intense. The control scheme does not alter these qualitative results. It must be noted that configurations f1 and f2 are not presented here, since they add no new information.

5.3. Comparison of control schemes

For the configuration shown in Fig. 12, the system is simulated for different control modes. Again the results are valid for all cases. Overall, the existence of active control yields a small jump to the reaction force, as compared to the uncontrolled (free-floating) case. This is explained by the fact, that, even if the impact happens for a fraction of time, it is still some non-zero time. Therefore, as the links start moving due to the impact, the controller tries to resist, and thus, reaction forces are created. This is the price to pay if one wants a controlled

position during an impact. The same happens when gearboxes are present at the joints. Generally it can be seen that gears create even higher reaction.

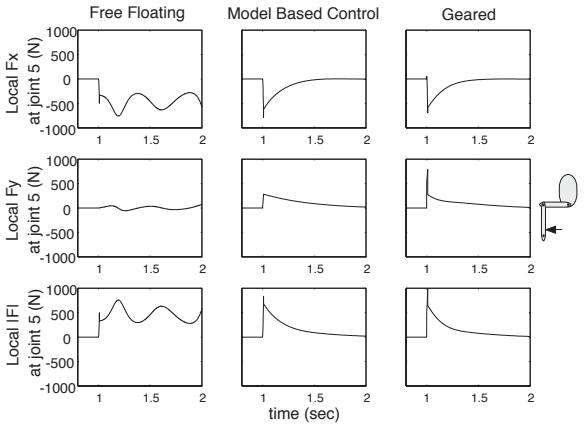

(a)

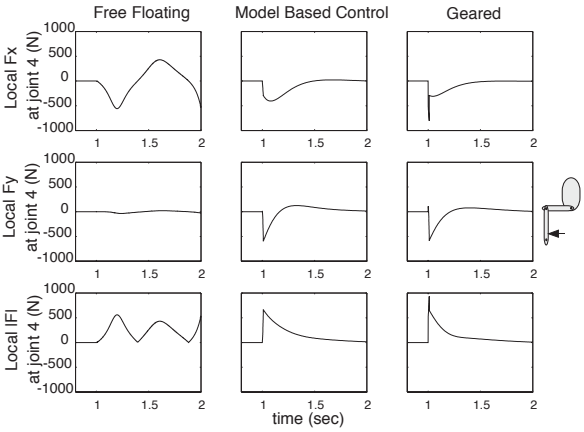

(b)

Figure 12. Different control schemes. Reaction force at joint (a) 5; (b) 4.

5.4. Maximum reaction force

A number of plots have been created, by measuring the maximum force that is exerted at the joints within the time of impact. The configurations shown in Fig. 9a and 9d have been examined thoroughly. As it can be seen in Fig. 13, the existence of active control increases reactions, but the minimum still occurs at the COP. The existence of gears additionally moves the minimum away from the COP, and the greater the gear ratio is, the greater the distance from the COP is. The only result that showed a rather peculiar behavior was observed for the configuration in Fig. 9a. Observing the plots in Fig. 14, two conclusions can be drawn. First, the response of joint 5 is as expected, but joint 4 shows a more complicated behavior. Second, the minimum for joint 4 occurs when the impact at link 5 is at different position than its COP. This is explained as follows.

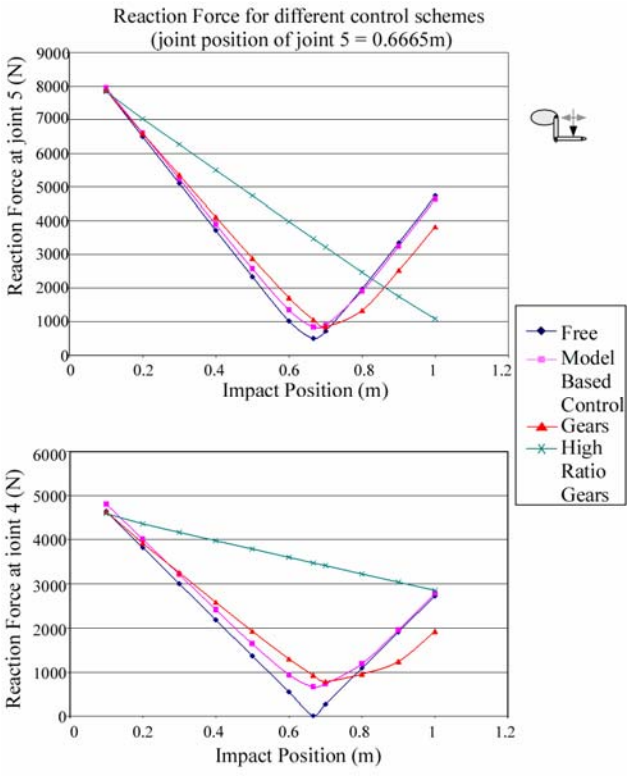

Figure 13. Reaction forces in relation with impact position. Comparison for different control schemes.

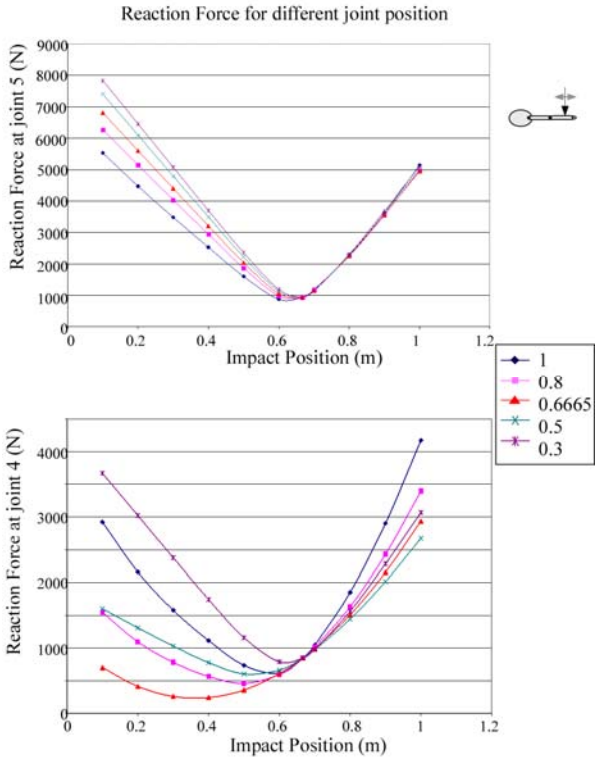

Figure 14. Reaction forces in relation with impact position. Comparison for different position of joint 5.

At the time of the impact, the system can be thought as a system with fixed joints. Joint 5 sees only link 5, therefore the results follow the theory. However joint 4 here, sees a fictional link consisted of links 4 and 5. In other words it sees a longer link, and by therefore the physical properties it sees are different. So the minimum occurs at another position, called the pseudo-COP. Although this seems interesting from an impact prospect, a number of problems arise. First, the impact must happen closer to joint 5 than to the COP. Even if joint 4 and the base are affected less, the reaction forces at joint 5 are large. Furthermore the uncertainties of an impact's position, impact angle or other system's uncertainties, are not filtered. If for example the impact angle is not 90^o the effects at the base are intense.

5.5. Impact Minimization Guidelines

The results of the previous studies can be summarized by the following guidelines:

- An impact should occur as near as possible to the measured COP and at 90^o angle. To this end, the robotic system must prepare itself for the impact.
- Revolute joints should be normal to each other, and connected at their COP at the moment of the impact.
- Two revolute joints for 2D cases and three revolute joints for 3D cases is the minimum of joints required for impact filtering.
- Given that the uncertainties cannot be predicted, the configuration with normal links gives the most well-behaved system, able to filter reaction forces better.

A final remark here is that whether it is better for the system to feel the impact as a free floating system, and have the control system take control later, or have the control system working continuously at a cost of higher reaction force, remains open and must be studied.

6. CONCLUSIONS

This work examined the behavior of a space robot at during an impact with a target. The strategy of planning an efficient docking and grasping of an object is examined to reduce the effects of impacts to the joints of the manipulator, and consequently to the base. What interests the most is how the physical concept of percussion point or center of percussion, which exists in all objects that can rotate around a fixed axis, can assist. An analysis of the COP and a number of simulations were developed in order to present the feasibility of the concept. Guidelines for the best configuration of a mechanism at time of impact were proposed. The study showed that by a clever configuration of the robotic system, the effects of an impact can be reduced largely, using only the manipulator's design and no additional hardware, realizing this way a natural filter.

ACKNOWLEDGEMENTS

Support of this work by the EPAN Cooperation Program 4.3.6.1.b (Greece-USA 035) of the Hellenic General Secretariat for Research and Technology is acknowledged.

REFERENCES

Waltz, Donald M., *On-Orbit Servicing of Space Systems*, Krieger Publishing Company, Florida, 1993.

Ellery, A., *An Introduction to Space Robotics*, Praxis Publishing Ltd, Chichester, UK, 2000.

Yoshida K., Nakanishi H., Ueno H., Inaba N., Nishimaki T. and Oda M., *Dynamics, Control and Impedance Matching for Robotic Capture of a Non-cooperative Satellite*, Advanced Robotics, Vol. 18, No. 2, 2004, pp. 175–198.

Jacobsen S., Lee C., Zhu C. and Dubowsky S., *Planning of Safe Kinematic Trajectories for Free Flying Robots Approaching an Uncontrolled Spinning Satellite,* Proceedings of DETC 2002, ASME 2002 Design Engineering Technical Conferences and Computer and Information in Engineering Conference, Montreal, Canada, September 29-October 2, 2002.

Martin E., Papadopoulos E. and Angeles J., *Control System Design for Reduced Thruster-Flexibility Interactions in Space Robots*, Proc. of the CSME Forum, Hamilton, ON, May 1996.

Carignan C. R. and Akin D. L., "*The Reaction Stabilization of On-Orbit Robots*, IEEE Control Systems Magazine, December 2000, pp. 15-18.

Papadopoulos E. and Dubowsky S., *Dynamic Singularities in the Control of Free-Floating Space Manipulators*, ASME Journal of Dynamic Systems, Measurement and Control, Vol. 115, No. 1, March 1993, pp. 44-52.

Papadopoulos E., Tortopidis I., and Nanos K., *Smooth Planning for Free-floating Space Robots Using Polynomials*, IEEE International Conference on Robotics and Automation (ICRA '05), April 2005, Barcelona, Spain, pp. 4283-4288.

Papadopoulos E., and Nanos K., *On Configuration Planning for Free-floating Space Robots*, Proceedings 15th CISM-IFToMM Symposium on Robot Design, Dynamics and Control, Montreal, Canada, June 14-18, 2004.